

## Energy Dependence of Electron Lifetime in Graphite Observed with Femtosecond Photoemission Spectroscopy

S. Xu,<sup>1</sup> J. Cao,<sup>2</sup> C. C. Miller,<sup>1</sup> D. A. Mantell,<sup>3</sup> R. J. D. Miller,<sup>1</sup> and Y. Gao<sup>2</sup>

<sup>1</sup>Center for Photoinduced Charge Transfer, Chemistry Department, University of Rochester, Rochester, New York 14627

<sup>2</sup>Department of Physics, University of Rochester, Rochester, New York 14627

<sup>3</sup>Webster Research Center, Xerox Corporation, Webster, New York 14580

(Received 18 August 1995)

The energy dependence of the electron lifetime in graphite was measured using femtosecond time-resolved photoemission spectroscopy. The lifetime was found to be inversely proportional to the excitation energy above the Fermi level, i.e.,  $(E - E_F)^{-1}$ , in sharp contrast to that of metals, whose lifetime is found to be proportional to  $(E - E_F)^{-2}$ . The results are in agreement with the prediction of the layered electron gas theory, which suggests that electron-plasmon interactions dominate the lifetime of electrons in a layered electron gas, even for small excitation energies, due to interlayer plasmon coupling.

PACS numbers: 72.15.Lh, 71.45.Gm, 73.61.Cw

The transient behavior of excited electrons in solids has been the subject of experimental and theoretical investigations for years. The finite lifetime of excited electrons reflects a number of decay channels, such as electron-electron, electron-plasmon, electron-phonon, electron-photon, and electron-impurity interactions. The elucidation of the relaxation channels provides insights into the basic interactions in many-body systems. The recent advent of ultrafast lasers has made it possible to probe dynamic processes in solids directly in the time domain on the femtosecond scale. Among time-resolved techniques, time-resolved photoemission spectroscopy (TR-PES) is unique in that it directly measures the temporal evolution of photoexcited electrons and the underlying microscopic process. Several TR-PES studies of metals [1–3] and semiconductors [4–8] have been reported. Notably, the TR-PES study on copper [1] showed the lifetime of the excited electrons close to the Fermi level is proportional to the inverse square of excitation energy, i.e.,  $(E - E_F)^{-2}$ . This result is expected from Fermi liquid theory [9–11] and reflects the fact that the dominant relaxation process near the Fermi level is electron-electron scattering. At energies higher than the plasmon energy, the electron-plasmon interaction becomes important and dominates the other decay channels [12].

In this Letter, the TR-PES investigation of the energy dependence of the electron relaxation lifetime in highly oriented pyrolytic graphite is reported. Graphite is viewed as a model system for layered electron gases, which can exist in many interesting materials such as layered compounds, semiconductor superlattices, and high temperature superconductors. The results show that the relaxation lifetime depends linearly on the inverse of the excitation energy referenced to the Fermi level, i.e.,  $\tau \propto (E - E_F)^{-1}$ . This is drastically different from what one would expect if electron-electron scattering were the dominant relaxation process, as in the case of copper, where

$\tau \propto (E - E_F)^{-2}$ . The theoretical analysis of the layered electron gas indicates that it is due to electron-plasmon interactions [13,14]. As far as we know, there has been no report of experimental evidence for electron-plasmon interaction in layered materials, whether in the time domain or frequency domain. Hence, these results on graphite provide the first experimental evidence that the dominant scattering process in layered materials can be electron-plasmon scattering, even for excitations close to the Fermi level.

The experimental setup has been described elsewhere [1]. The laser system consists of an Ar<sup>+</sup> laser pumped self-mode-locked Ti:sapphire laser, with a pulse width of  $\sim 43$  fs, a pulse energy of  $\sim 10$  nJ, a wavelength of  $\sim 750$  nm, and a repetition frequency of  $\sim 82$  MHz. The frequency-doubled pulse ( $h\nu = 3.31$  eV) was passed through a pair of external prisms for group-velocity dispersion compensation. A beam splitter was used to separate the frequency-doubled light into two beams, i.e., pump and probe beams, with equal intensity. The pulse width of the frequency-doubled light was measured to be 63 fs from the two pulse convolution of the photoemission spectrum of a stainless steel sample, on the assumption that its lifetime is negligible far above the Fermi level ( $>3.0$  eV).

The ultrahigh vacuum system has a base pressure of  $5 \times 10^{-11}$  torr. A highly oriented pyrolytic graphite sample was cleaved *in situ* to obtain a clean surface (0001). It was set at  $45^\circ$  relative to the laser beam and normal to the entrance axis of the energy analyzer. The energy analyzer has a resolution of 200 meV. In order to eliminate the effects of any stray electric fields and extend the range of  $\mathbf{k}$  states being collected, a  $-10.0$  eV bias is applied to the sample. A small amount of Cs was deposited to lower the work function of graphite so that we could measure the data close to the Fermi level. The work function change can be obtained from the extension of the emission cutoff,

which gives the work function of Cs-deposited graphite in our experiment to be 3.66 eV. The deposited Cs, less than  $4 \times 10^{13}$  atoms/cm<sup>2</sup> as estimated [15] from the work function change of  $-1.04$  eV, covers only less than 0.1 monolayer on the graphite surface, with little or no effects on the inner graphite layers. Experimentally, we observed that the photoemission spectra were extended only to the low kinetic energy side without any noticeable change on the high kinetic energy side when Cs was deposited [see Fig. 1(b)], indicating little change of the electronic properties in the range of interest.

The schematic diagram of the two-photon photoemission process is shown in Fig. 1(a), and in Fig. 1(b), the photoemission spectrum of pristine graphite (dash line) and Cs-covered graphite (solid line), measured with one of the laser beams blocked, are shown. The broad features of the spectrum indicate that, besides the direct transition (that is,  $\Delta k_{\parallel} = 0$ ), the indirect transition (that is,  $\Delta k_{\parallel} \neq 0$ ) can also happen due to phonon assistance [16]. Further analysis shows the signal intensity varies quadratically with laser power, as expected for a two-photon process. The time-resolved photoemission experiment was carried out by monitoring the number of electrons at a given kinetic energy as a function of delay between the two pulses, i.e., pump and probe pulses. The scan obtained when monitoring photoelectrons at a kinetic energy of 1.69 eV is shown in the inset of Fig. 2.

Generally the two-photon process contains two channels [17]. In the simultaneous channel, the two-photon transition is due to the absorption of two photons simulta-

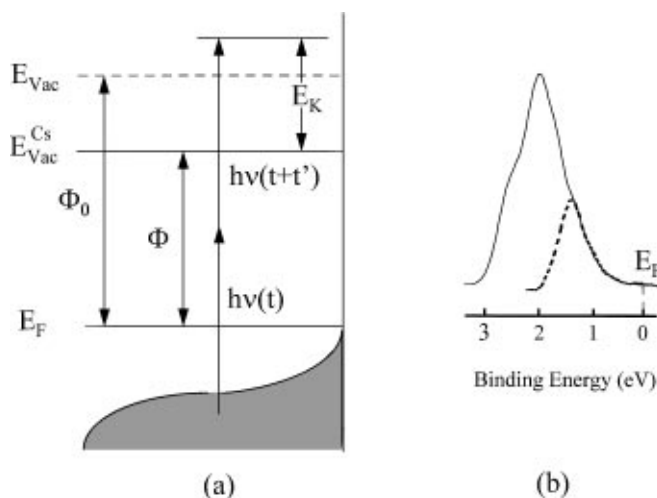


FIG. 1. (a) The schematic representation of the two-photon photoemission process. The shaded region indicates the density of occupied states, where  $E_K$  is the kinetic energy of the photoelectron,  $E_{\text{Vac}}$  and  $E_{\text{Vac}}^{\text{Cs}}$  are the vacuum level of graphite without and with Cs deposition, respectively,  $\Phi_0$  and  $\Phi$  are the work function without and with Cs deposition, respectively,  $h\nu$  is the photon energy, and  $t'$  is the time delay between the pump pulse and the probe pulse. (b) The photoemission spectra of the Cs-covered graphite (solid line) and pure graphite (dash line) obtained with one beam blocked, where  $E_F$  is the Fermi level.

neously and has nothing to do with the population of the intermediate states. In the sequential channel, on the other hand, the electron is first excited to an intermediate state by the pump pulse and is photoemitted from the intermediate state by the probe pulse. In order to eliminate the simultaneous two-photon process, we employed a pair of crossed-polarized laser pulses with the pump beam  $p$  polarized and the probe  $s$  polarized, as demonstrated in our previous results [18]. In this case, the line shape of the pump-probe scan is the convolution of the autocorrelation function of the two laser pulses and the exponential decay function of the conduction band electrons,  $\exp(-|t|/\tau)$ , where  $\tau$  is the relaxation lifetime of the conduction band electron [1,18]. By fitting the experimental data with the convoluted function, the lifetime of the conduction band electron was extracted. The variation of lifetime with respect to the excitation energy is shown in Fig. 2, where the excitation energy relative to the Fermi level was calculated with the value of the work function  $\Phi$ , the photon energy of the probe laser  $h\nu$ , and the kinetic energy of photoelectron  $E_K$ , i.e.,  $E - E_F = E_K + \Phi - h\nu$  [Fig. 1(a)]. Since the lifetime measurement was done beyond 0.3 eV above the Fermi level and the lifetimes measured are all below 100 fs, it is unnecessary to consider the cascade of high energy electrons into lower energy states. Also the transport effect is small for graphite due to its layered nature, so the deconvoluted times should accurately represent the excited electron lifetime.

Compared with the results obtained in the copper experiment, we found that the lifetime of conduction band electrons in graphite had nearly the same magnitude as observed in copper, whose lifetime is mainly due to the

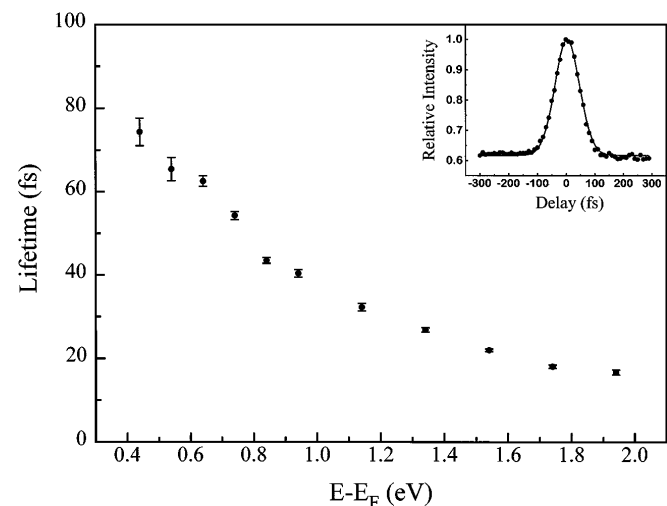


FIG. 2. Experimentally measured relaxation lifetimes of conduction band electrons are plotted as a function of energy relative to the Fermi level, i.e.,  $E - E_F$ . The inset shows the pump-probe scan when monitoring electrons with  $E_K = 1.69$  eV, where the filled circles are the experimental data while the solid line is the fitting given by the convolution of the autocorrelation function of the two pulses and the exponential decay function of the conduction band electrons.

electron-electron scattering process. This is somewhat surprising since electron-electron scattering in graphite should be very small because graphite is a semimetal with a pointed Fermi surface [19]. From Zunger's calculation, the density of states near the Fermi level is small and vanishes at the Fermi level [20]. This greatly reduces the chance of electron-electron scattering according to Fermi liquid theory [11,12]. Another factor diminishing the chance of electron-electron scattering is the geometric confinement of charge carriers since the excited electrons can be scattered only by the electrons in the same graphite layer. Those in other layers have no effect. Both factors would have led to longer lifetimes if electron-electron scattering were the main decay channel.

A close inspection of the energy dependence of the relaxation lifetime shows a fundamental difference between the copper and the graphite. The least-squares fitting of the graphite data shows that  $\ln(1/\tau)$  vs  $\ln(E - E_F)$  gives a slope of 1.07 (see the solid line in Fig. 3). This suggests the inverse lifetime is linearly proportional to the excitation energy referenced to the Fermi level, i.e.,  $\tau^{-1} \sim (E - E_F)$  (see the inset in Fig. 3). This result is in sharp contrast to  $\tau^{-1} \sim (E - E_F)^2$  observed in Cu, a three-dimensional (3D) metal and dictated by Fermi liquid theory.

A semiquantitative description of the excitation energy above the Fermi level has been obtained by treating the

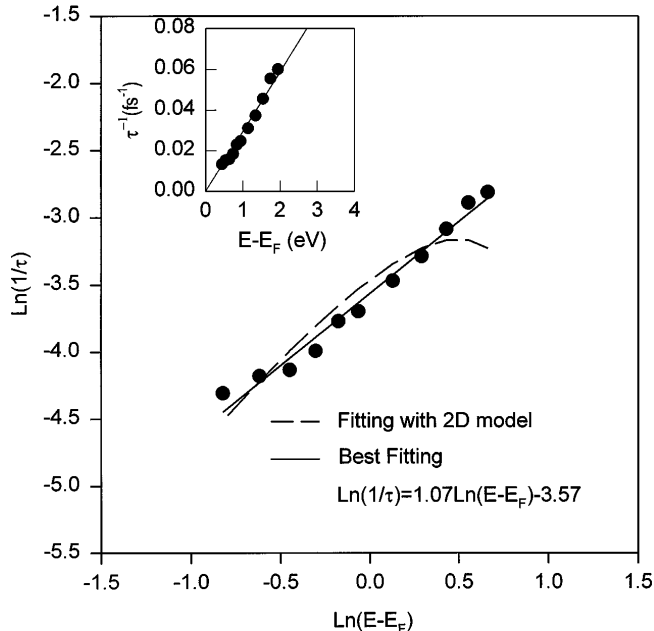


FIG. 3. Logarithmic plot of the inverse lifetimes of photoexcited conduction band electrons vs their energy relative to the Fermi level, i.e.,  $E - E_F$ . The filled circles are the experimental data, while the solid line is the least-squares fit with the layered electron gas model. The dashed line shows the fit with the 2D electron gas model. The inset shows a linear scale plot of the inverse lifetime vs the excitation energy, where the filled circles stand for experimental data, and the solid line stands for the prediction of the layered electron gas theory.

excitation as a “quasiparticle” [10]. The self-energy of the quasiparticle contains an imaginary part which reflects the relaxation of the excited electron. Within the random-phase approximation, the imaginary part of the self-energy consists of two terms, i.e., the excitation of another electron-hole pair (corresponding to electron-electron scattering) and plasmons (electron-plasmon scattering) [21]. For the quasiparticle close to the Fermi surface, i.e.,  $k \sim k_F$ , only the excitation of electron-hole pairs contribute to the lifetime in a 2D or 3D electron gas [13]. The lifetime of excited electrons in a 2D electron gas at low excitation energy can be written as [21]

$$\frac{1}{\tau_{ee}} = -\frac{E_F}{4\pi\hbar} \left[ \frac{E - E_F}{E_F} \right]^2 \times \left[ \ln\left(\frac{E - E_F}{E_F}\right) - \frac{1}{2} - \ln\left(\frac{2q_{TF}^{(2)}}{p_F}\right) \right], \quad (1)$$

where  $\tau_{ee}$  is the lifetime due to the electron-electron scattering,  $E_F$  and  $p_F$  are the Fermi energy and Fermi wave vector, respectively, and  $q_{TF}^{(2)}$  is the Thomas-Fermi screening wave vector in 2D given by  $2me^2/\hbar^2$ . The fitting with Eq. (1) has been done for graphite, and the fitting results are plotted in Fig. 3. The fit is poor and cannot explain the trend of the experimental data. This leads us to dismiss electron-electron scattering as the main decay channel and to search for an alternative many-body interaction mechanism to explain the graphite data.

In 3D metals, electron-plasmon interactions become dominant for the excitation energies above a critical value [12]. Nevertheless, electron-plasmon interactions cannot happen in 3D or 2D systems when the excitation energy  $\xi_k$  is less than the critical value  $\Delta_C$ , which is usually a large fraction of the Fermi energy. In 3D systems, the plasmon spectrum is almost nondispersive, and the threshold value  $\Delta_C$  is  $\hbar\omega_P$ , the plasmon energy [13,14]. Although the 2D plasmon spectrum is dispersive ( $\omega_P^2 \propto q$ , for small  $q$ 's), a kinematic constraint prohibits the electrons of low excess energy from transferring their energy to plasmons [13,14,21].

The layered nature makes the excited electrons in the layered material quite different from that in a 2D or 3D system, and the layered electron gas (LEG) model [13,14] is needed to describe the many-body interactions in this system. Unlike a 3D and 2D electron gas, LEG is an inhomogeneous and highly anisotropic medium. The electrons in the layered electron gas can move freely in the two-dimensional electron gas layers, while motion between the layers is forbidden. Nevertheless, the plasmons associated with the individual layers couple with each other through long-range Coulomb interactions, leading to the formation of a plasmon band [13,14,22]. Because of the formation of this band, electron-plasmon interactions become an effective channel for excited electron relaxation, even at small excitation energies. The smaller the interlayer separation, the larger the band width

will be in phase space [14]. The formation of the plasmon band reduces the kinematic constraints for the electron-plasmon interactions close to the Fermi level, and hence, plasmon excitation becomes an effective channel for the relaxation of excited electrons even for low excitation energy. Generally, electron-electron scattering is very weak in a LEG due to the geometric confinement of the 2D charge carrier [18]. Hence, when the interlayer separation is small, as is the case of graphite, the electron-plasmon interactions can dominate the excited electron lifetime [14]. In this case, the lifetime of an excited electron can be written as [14]

$$\tau_k^{-1} = \frac{8\mathfrak{R}\sqrt{a}}{\sqrt{2}r_s^2} \left[ \frac{1 + 1/a}{(1 + 1/a)^2 - 1} \right]^{3/2} \left[ \frac{k - k_F}{k_F} \right]^2, \quad (2)$$

where  $\mathfrak{R}$  is the effective Rydberg constant in units of  $\hbar$ ,  $a$  is the interlayer separation, and  $r_s$  is the average distance between electrons in the layer. Both  $a$  and  $r_s$  are measured in units of effective Bohr radius  $a_0$ .

For excitation close to the Fermi level, we have

$$\tau_E^{-1} \approx C(E - E_F), \quad (3)$$

where  $E_F$  is the Fermi energy and

$$C = \frac{8\mathfrak{R}\sqrt{a}}{\sqrt{2}r_s^2 E_F} \left[ \frac{1 + 1/a}{(1 + 1/a)^2 - 1} \right]^{3/2}. \quad (4)$$

That is to say, the inverse lifetime is proportional to the excitation energy referenced to the Fermi level. For graphite, the interlayer separation is 3.37 Å [23] and the effective mass near the Fermi level is  $0.06m_e$  [24]. Hence  $a$  and  $\mathfrak{R}/\hbar$  are calculated to be 0.38 and 1.24 fs<sup>-1</sup>, respectively. For electrons in 2D layers,  $r_s$  and  $k_F$  are related to the electronic density  $n$  by [12]

$$n = k_F^2/2\pi \quad (5)$$

and

$$1/n = \pi r_s^2. \quad (6)$$

Consequently,  $E_F$  can be calculated as [12]

$$E_F = (27.2 \text{ eV})/r_s^2. \quad (7)$$

Putting them together into Eq. (4) gives  $C = 0.026 \text{ eV}^{-1} \text{ fs}^{-1}$ . This value is in excellent agreement with the best fit to the experimental data which gives  $0.029 \text{ eV}^{-1} \text{ fs}^{-1}$  (Fig. 3). The degree of agreement between the layered electron gas theory and our time-resolved lifetime measurements for graphite gives direct experimental evidence that electron relaxation in graphite is mainly due to the electron-plasmon interaction.

Although our observation is based on graphite, the result can be applied to other layered compounds including semiconductor superlattices since the dominant contribution of the electron-plasmon interaction to the electron relaxation is due to the layered nature of graphite. The fact that graphite has a point Fermi surface may also con-

tribute to the insignificance of electron-electron scattering and dominance of electron-plasmon scattering observed. Nonetheless, the layered nature alone can also greatly reduce the electron-electron scattering since the electron-electron interaction can happen only inside each layer and its contribution to the 2D electron relaxation is about 3–4 times slower than that of 3D electron relaxation [18].

Finally, we believe our results on graphite may have significant implications for the case of high- $T_c$  superconductors. Recent studies [25] on line broadening in angle-resolved photoemission spectra of Bi<sub>2</sub>Sr<sub>2</sub>CaCu<sub>2</sub>O<sub>8</sub> show that the effective inverse photohole lifetime is linear in energy. This has been presented as evidence that the electron system in high temperature superconductors is a non-Fermi-liquid. From our results, we believe that these phenomena may also be caused by the electron-plasmon interaction as in graphite, since Bi<sub>2</sub>Sr<sub>2</sub>CaCu<sub>2</sub>O<sub>8</sub> as well as most other high- $T_c$  superconductors have a layered electronic structure [25].

The authors would like to thank M. Aeschlimann for helpful discussions. This work is supported by National Science Foundation Grant No. CHE-9120001.

- 
- [1] C. A. Schmuttenmaer *et al.*, Phys. Rev. B **50**, 8957 (1994).
  - [2] R. W. Schoenlein *et al.*, Phys. Rev. Lett. **61**, 2596 (1988).
  - [3] W. S. Fann *et al.*, Phys. Rev. Lett. **68**, 2834 (1992).
  - [4] R. Haight *et al.*, Phys. Rev. Lett. **54**, 1302 (1985).
  - [5] J. Bokor *et al.*, Phys. Rev. Lett. **57**, 881 (1986).
  - [6] N. J. Halas and J. Bokor, Phys. Rev. Lett. **62**, 1679 (1989).
  - [7] J. R. Goldman and J. A. Prybyla, Semicond. Sci. Technol. **9**, 694 (1994).
  - [8] R. Haight and M. Baeumler, Surf. Sci. **287/288**, 482 (1993).
  - [9] J. J. Quinn, Phys. Rev. **126**, 1453 (1962).
  - [10] D. Pines and P. Nozieres, *The Theory of Quantum Liquids* (Benjamin, New York, 1966).
  - [11] N. W. Ashcroft and N. D. Mermin, *Solid State Physics* (Holt, Rinehart and Winston, New York, 1976).
  - [12] M. P. Seah and W. A. Pench, Surf. Interface Anal. **1**, 2 (1979).
  - [13] P. Hawrylak, Phys. Rev. Lett. **59**, 485 (1987).
  - [14] P. Hawrylak *et al.*, Phys. Rev. B **37**, 10 187 (1988).
  - [15] Z. P. Hu *et al.*, Surf. Sci. **177**, L956 (1986).
  - [16] F. J. Himpsel, Adv. Phys. **32**, 1 (1983).
  - [17] S. H. Lin *et al.*, *Multiphoton Spectroscopy of Molecules* (Academic Press, New York, 1984).
  - [18] C. A. Schmuttenmaer *et al.*, J. Chem. Phys. (to be published).
  - [19] A. Santoni *et al.*, Appl. Phys. A **52**, 299 (1991).
  - [20] A. Zunger, Phys. Rev. B **17**, 626 (1978).
  - [21] G. F. Giuliani and J. J. Quinn, Phys. Rev. B **26**, 4421 (1982).
  - [22] R. Sooryakumar *et al.*, Phys. Rev. B **31**, 2578 (1985).
  - [23] R. F. Willis *et al.*, Phys. Rev. B **4**, 2441 (1971).
  - [24] R. C. Tatar and S. Rabii, Phys. Rev. B **25**, 4126 (1982).
  - [25] C. G. Olson *et al.*, Phys. Rev. B **42**, 381 (1990).